

## On Restoration of Degraded Fingerprints

Indu Joshi<sup>1</sup> · Ayush Utkarsh<sup>2</sup> · Pravendra  
Singh<sup>3</sup> · Antitza Dantcheva<sup>4</sup> · Sumantra  
Dutta Roy<sup>1</sup> · Prem Kumar Kalra<sup>1</sup>

Received: date / Accepted: date

**Abstract** The state-of-the-art fingerprint matching systems achieve high accuracy on good quality fingerprints. However, degraded fingerprints obtained due to poor skin conditions of subjects or fingerprints obtained around a crime scene often have noisy background and poor ridge structure. Such degraded fingerprints pose problem for the existing fingerprint recognition systems. This paper presents a fingerprint restoration model for a poor quality fingerprint that reconstructs a binarized fingerprint image with an improved ridge structure. In particular, we demonstrate the effectiveness of channel refinement in fingerprint restoration. The state-of-the-art channel refinement mechanisms, such as Squeeze and Excitation (SE) block, in general, create SE-block introduce redundancy among channel weights and degrade the performance of fingerprint enhancement models. We present a lightweight attention mechanism

---

Indu Joshi  
E-mail: indu.joshi@cse.iitd.ac.in

Ayush Utkarsh  
E-mail: ayushutkarsh@gmail.com

Pravendra Singh  
E-mail: psingh@iitk.ac.in

Antitza Dantcheva  
E-mail: antitza@inria.fr

Sumantra Dutta Roy  
E-mail: sumantra@ee.iitd.ac.in

Prem Kumar Kalra  
E-mail: pkalra@cse.iitd.ac.in

<sup>1</sup> Indian Institute of Technology Delhi, India

<sup>2</sup> Independent Researcher, India

<sup>3</sup> Indian Institute of Technology Kanpur, India

<sup>4</sup> Inria Sophia Antipolis, France

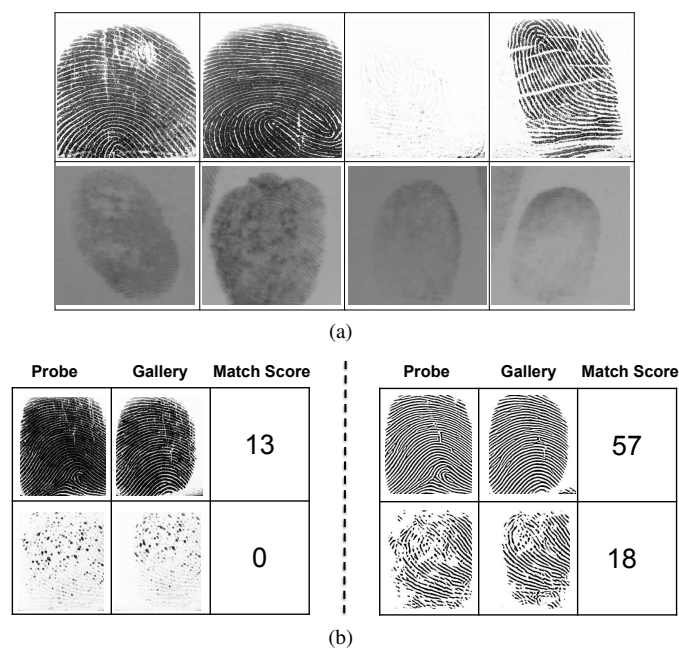
that performs channel refinement by reducing redundancy among channel weights of the convolutional kernels. Restored fingerprints generated after introducing proposed channel refinement unit obtain improved quality scores on standard fingerprint quality assessment tool. Furthermore, restored fingerprints achieve improved fingerprint matching performance. We also illustrate that the idea of introducing a channel refinement unit is generalizable to different deep architectures. Additionally, to quantify the ridge preservation ability of the model, standard metrics: Dice score, Jaccard Similarity, SSIM and PSNR are computed with the ground truth and the output of the model (CR-GAN). An ablation study is conducted to individually quantify the improvement of generator and discriminator sub-networks of CR-GAN through channel refinement. Experiments on the publicly available IITD- MOLF, Rural Indian Fingerprint Database and a private rural fingerprint database demonstrate the efficacy of the proposed attention mechanism.

**Keywords** Fingerprints · Restoration · Denoising · Biometrics · Deep convolutional neural networks

## 1 Introduction

Accurate matching performance of fingerprints-based authentication systems promotes their usage in various applications ranging from border security, access control to law enforcement. However, poor quality fingerprint images resulting due to aging, dry/wet fingers, creases, or uncontrolled interaction of the subjects with the fingerprint sensors adversely affect the performance of the state-of-the-art fingerprint matching systems [1][2]. Furthermore, the rural population of developing countries often has poor fingertip skin quality due to the large amount of manual work. As a result, state-of-the-art fingerprint minutiae extractors fail to correctly extract minutiae on degraded rural fingerprints, leading to unsatisfactory matching performance. Some fingerprints are degraded due to the very nature of their acquisition, e.g., latent fingerprints. Latent fingerprints are collected from a crime scene and have poor ridge structure accompanied by structured noise. The structured noise in a latent fingerprint may exist due to stains, lines, overlapping text, and many times overlapping fingerprints in the background. Sample degraded fingerprints are shown in Figure 1 (a). To overcome the challenges offered by degraded fingerprints, its restoration is primarily performed via an *enhancement* model. An enhancement model is targeted to remove background noise, improve the contrast between ridges and valleys and predict missing ridge details. As a result, enhanced fingerprint image helps accurate minutiae extraction and improved fingerprint matching performance (see Figure 1 (b)).

State-of-the-art fingerprint enhancement models employ convolutional neural networks (CNNs) as the backbone architectures. However, studies indicate that deep architectures often learn redundant features [3][4]. Channel refinement is a state-of-the-art technique to improve the representational power of a CNN by facilitating learning of robust features. It has been successfully applied in image classification, scene classification and object detection [3] [4]. Unlike natural images, the training datasets in the fingerprint domain are relatively very small. The state-of-the-art



**Fig. 1** (a) Sample fingerprints from publicly available databases used in this research: first row- Rural Indian Fingerprint Database [5] depicting dry, wet fingerprint images and fingerprints with degraded ridges due to warts, scars, and creases. Second row- IIITD- MOLF Database [6] illustrating challenges such as background noise, unclear ridge details, and overlapping fingerprints in the background (b) left column showcases the match score between original probe and gallery fingerprints obtained using standard fingerprint matching tool NBIS [7] while the right column showcases the higher matching score obtained on the enhanced images generated by the proposed CR-GAN.

channel refinement technique SE-block [3] introduces a large number of additional model parameters into the architecture of fingerprint enhancement model. We observe that SE-block introduces redundancy among channel weights and degrades the performance of fingerprint enhancement models. To address the limitations of SE-block, this paper proposes a lightweight channel-level attention mechanism (referred as channel refinement unit) which refines the channel weights learnt by a deep learning based enhancement model. We show that channel refinement reduces redundancy among channel weights of fingerprint enhancement models and helps to learn robust features. Learning of robust features helps the enhancement model localize the fingerprint ridge pixels better, facilitating improved minutiae extraction and fingerprint matching performance. To the best of our knowledge, this is the first work to demonstrate the effectiveness of channel refinement in fingerprint enhancement.

## Research Contributions

The contribution of this research is six folds:

- We benchmark the performance of state-of-the-art fingerprint enhancement models on a publicly available Rural Indian Fingerprint database and a private rural Indian fingerprint database and demonstrate that the proposed approach significantly outperforms the state-of-the-art.
- The effectiveness of Squeeze and Excitation (SE) block [3] is studied by introducing SE block into a state-of-the-art fingerprint enhancement model. Visualizations of correlation matrices show that SE block creates redundancy among channel weights and does not generalize for fingerprint reconstruction. However, the proposed channel refinement unit successfully reduces redundancy among channel weights.
- Generalization performance of proposed channel refinement on different deep architectures is demonstrated.
- A detailed comparison with state-of-the-art generative adversarial network based fingerprint enhancement models showcasing the superior performance of the proposed CR-GAN is given.
- Ablation study is conducted to gain insights on the effectiveness of introducing channel refinement in the network architecture.
- Superior performance achieved on challenging fingerprint databases of the rural Indian population and a latent fingerprint database demonstrate the generalization ability of the proposed work.

## 2 Related Work

### 2.1 Attention Mechanisms

Attention is a means to influence the network parameters of a CNN to focus on the most informative components of the input. Attention mechanisms in CNNs are motivated by the human visual system. Humans do not process the whole scene at once, rather sequentially in partial glimpses. Similarly, attention mechanisms are designed to empower the CNN architectures to identify salient features and improve its representational power [8] [9]. Next, we summarize state-of-the-art attention mechanisms proposed in the literature.

Squeeze and Excitation (SE) block [3] is one of the most widely used attention mechanisms. It understands the relationship between channels and adapts the features such that inter-dependencies among channels are taken care of. [4] and [10] are concurrent works which exploit both spatial and channel level information. The authors propose spatial attention and a channel attention module. Recalibrated features from both the modules are fused to obtain the final output feature map. Hu *et al.* [11] modify the squeeze operation of SE-block and propose Gather-Excite block. The gather operation performs a parameterized aggregation of feature responses while the excitation operation is similar to excite operation of SE-block. Huang *et al.* propose criss-cross attention [12] to capture contextual information in images. Singh *et al.* [13] propose calibration of features through attention weights. Bello *et al.* [14] propose to augment convolution operations with self-attention to improve a model's performance.

Attention mechanisms are successfully utilized in many applications including image classification, sequence learning, object detection, image captioning and scene classification [3] [4] [15] [16]. Motivated by the success of attention mechanisms in image processing and computer vision applications [17] [18] [19], we propose a lightweight channel refinement mechanism for improving the feature representations of fingerprint images. The proposed channel refinement unit is similar to the SE-block [3]. However, SE-block performs redundant transformations, which not only introduces additional parameters but also creates redundancy across features. A detailed comparison between SE-block and the proposed channel refinement unit is provided in Section 5.3.

## 2.2 Fingerprint Enhancement

Vatsa *et al.* [20], Puri *et al.* [5], and Tiwari *et al.* [21] assess the fingerprint quality of the rural Indian population. These studies conclude that the fingerprint quality of the rural Indian population is poor. Furthermore, these studies also report the unsatisfactory performance of the state-of-the-art fingerprint matching systems on the rural Indian population. While the challenges in the rural fingerprint matching have been identified, the effectiveness of fingerprint enhancement models on the rural population has not been established so far. We now summarize the literature on the enhancement of poor quality fingerprints, in general, below.

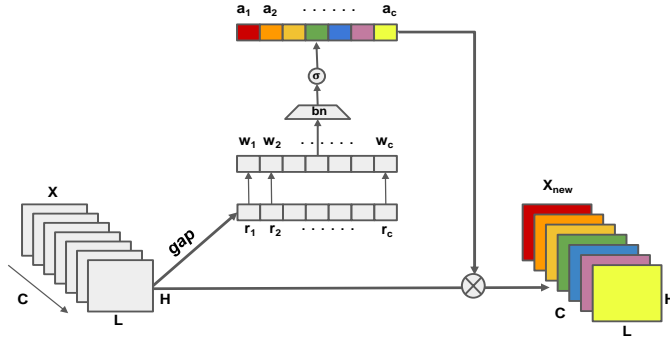
**Classical image processing techniques based enhancement:** Hong *et al.* [22] propose computation of ridge orientation and frequency on normalized fingerprint images. Enhanced image is obtained by applying Gabor filters tuned to the computed orientation and frequency. Gottschlich and Schönlieb [23], Turrone *et al.* [24], Ramos *et al.* [25], Wang *et al.* [26] and Gottschlich [27] propose contextual filtering of fingerprint images in spatial domain. Chikkerur *et al.* [28] propose short time Fourier transform (STFT) to obtain the local ridge orientation and frequency. The obtained contextual information is used to filter the fingerprint image. Hsieh *et al.* [29] propose wavelet transform based fingerprint image enhancement. Ghafoor *et al.* [30] propose Fourier and spatial domain based contextual filtering for fingerprint enhancement. Jirachaweng and Areekul [31] propose discrete cosine transform based fingerprint enhancement. Yoon *et al.* [32] propose zero pole and distortion model for orientation estimation to perform fingerprint enhancement. Gupta *et al.* [33] exploit density of minutiae and direction of orientation field through a high order polynomial for reconstructing a poor quality fingerprint image. Le *et al.* [34] propose adaptive singular value decomposition of wavelet sub-bands to discard noisy background and improve the clarity of fingerprint ridge patterns. Manickam *et al.* [35] improve contrast of fingerprint images using type-2 fuzzy sets and extract scale invariant feature transform (SIFT) feature points. Later, the authors SIFT feature points to match fingerprints.

**Learning based enhancement techniques:** Yang *et al.* [36] propose localized dictionaries for fingerprint enhancement. Chen *et al.* [37] propose multi-scale dictionaries based fingerprint enhancement. Liu *et al.* [38] propose multi-scale sparse coded dictionaries for enhancement. Xu *et al.* [39] learn multi-scale dictionaries and exploit principal component analysis (PCA) for reducing dimensionality of dictio-

naries. Fingerprint image is enhanced using these dictionaries and spectra diffusion. Sahasrabudhe and Namboodiri [40] propose deep belief networks for enhancement of fingerprints. Schuch *et al.* [41] propose a deconvolutional autoencoder (DeConvNet) for enhancement of fingerprint images. Reddy KNV and Namboodiri [42] propose hierarchical markov random field based filtering. Svoboda *et al.* [43] propose an autoencoder network which minimizes gradient and orientation between the output and target enhanced image. Horapong *et al.* [44] propose a spectral autoencoder based feedback mechanism to identify anomalously enhanced fingerprint regions. The poorly enhanced regions are iteratively enhanced to improve quality of fingerprint ridge patterns. Qian *et al.* [45] propose DenseUnet based fingerprint enhancement. Liu and Qian *et al.* [46] propose a nested Unet based architecture that optimizes a combination of local and global losses for segmentation and enhancement of poor quality fingerprint images. Wong and Lai [47] and Li *et al.* [48] propose multi-tasking autoencoder which enhances fingerprint image while also predicting orientation details. Sharma and Dey [49] propose a quality adaptive fingerprint enhancement algorithm which first assesses the quality of a fingerprint image and then applies quality adaptive pre-processing. Finally, the pre-processed image is enhanced through standard enhancement algorithms. Joshi *et al.* [50] propose to incorporate model uncertainty into an existing fingerprint enhancement model to assess confidence of the fingerprint enhancement model. Medeiros *et al.* [51] propose a convolutional neural network to select the best enhancement model for a given poor quality fingerprint image. Fingerprint enhancement methods have been revisited by Schuch *et al.* [52].

Joshi *et al.* [53] [54] propose a generative adversarial network (GAN) based fingerprint enhancement algorithm (FP-E-GAN) and show its superior performance. Karabulut *et al.* [55] propose a cycle-consistent GAN for unpaired translation from distorted domain to non-distorted domain. Recently, Joshi *et al.* [56] propose to introduce data uncertainty in fingerprint enhancement models and show that data uncertainty guided GAN (DU-GAN) outperforms state-of-the-art fingerprint enhancement models. GAN is the state-of-the-art architecture for image generative applications. Therefore, such an approach constitutes a promising architecture for fingerprint enhancement. However, fingerprint images have minor intensity variations compared to natural images. We hypothesize that it is highly likely that many of the channel weights (of the convolutional kernels) learnt by the GAN might be redundant and may not contribute to fingerprint enhancement.

In this paper, we take FP-E-GAN [53] as the backbone network and introduce the proposed channel refinement unit into it and fabricate a novel architecture: **CR-GAN**. The proposed channel refinement unit ensures that different salient features are learnt by the model, and redundancy among channel weights is reduced. We demonstrate that smoother enhanced images with lesser artifacts are generated after the introduction of the channel refinement unit, and improved matching performance is obtained.



**Fig. 2** The proposed channel refinement unit (CRU) refines the channel weight vector  $X$  to  $X_{new}$ . CRU reduces redundancy among channel weights and ensures that relevant features are learnt by the fingerprint enhancement model. The adversarial training of CR-GAN ensures that the enhanced image output by the generator network preserves ridge structure and does not have artifacts.

### 3 Proposed Model

We approach fingerprint enhancement as an image-to-image translation problem. The enhancement model is trained to remove noise and output a binarized fingerprint image with improved ridge-valley details.

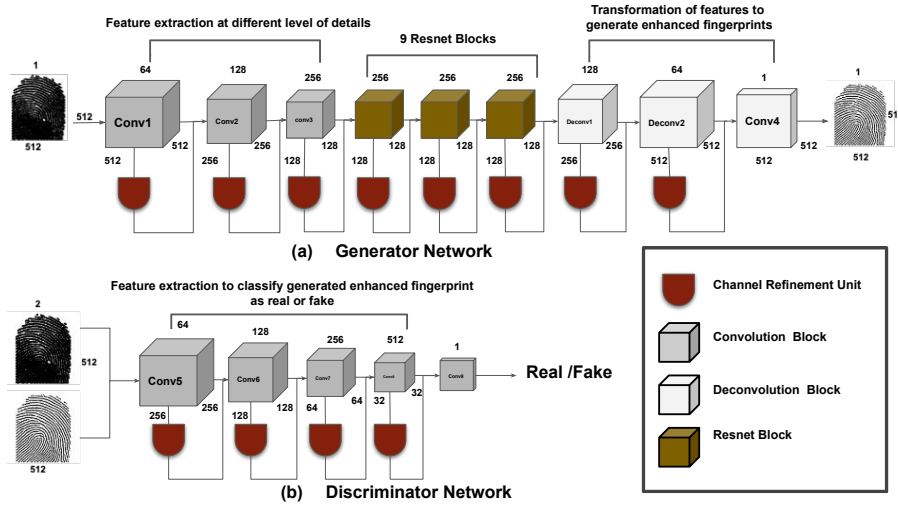
#### 3.1 Channel Refinement Unit:

Given an input tensor  $X \in R^{L \times H \times C}$ , the channel refinement unit (CRU) generates an output tensor  $X_{new}$  with refined values, as shown in Figure 2. Convolution operators extract local features corresponding to their receptive field. However, to assess the effectiveness of each channel towards fingerprint enhancement, global information originating from the overall activation over the fingerprint image is required. To obtain the global representation ( $Rep$ ) of each of the  $C$  channels in a convolution block, CRU has a global average pooling ( $gap$ ) layer which takes the average of all the activations corresponding to each channel, resulting in a  $C$  dimensional tensor,  $Rep=[r_1, r_2, \dots, r_C]$  where  $r_i \in R$ .

To understand the relative importance of each of the  $C$  channels,  $C$ ,  $1 \times 1$  depth wise convolution ( $dwc$ ) operations are performed resulting in an output  $W=[w_1, w_2, \dots, w_C]$ , where  $w_i \in R$ . The refined weights are obtained after applying batch normalization ( $bn$ ) and sigmoid ( $\sigma$ ) activation on  $W$ , giving an output tensor  $A=[a_1, a_2, \dots, a_C]$  ( $a_i \in R$ ), which has refined weights for each channel. The refined output  $X_{new}$  is the element wise product of the input  $X=[x_1, x_2, \dots, x_C]$  (where  $x_i \in R^{W \times H}$ ) with the corresponding refined channel weight.

$$A = \sigma(\text{bn}(\text{dwc}(\text{gap}(X))))$$

$$X_{new} = [x_1 \cdot a_1, x_2 \cdot a_2, \dots, x_C \cdot a_C]$$



**Fig. 3** Flowchart illustrating the network architecture of the proposed CR-GAN. The generator sub-network generates an enhanced binarized fingerprint image while the discriminator sub-network classifies it as real or fake.

### 3.2 Network Design of CR-GAN

Figure 3 depicts the network architecture of the proposed CR-GAN. The generator has an autoencoder architecture. The encoder sub-network of the generator learns noise-invariant features, which the decoder sub-network learns to convert into a high-quality binarized fingerprint image. The backbone network, training loss, and other hyperparameters are adopted from the state-of-the-art generative adversarial network-based fingerprint enhancement model [53]. We introduce a channel refinement unit after the convolutional blocks in both the generator and the discriminator. This fabricates a novel architecture: CR-GAN.

The network architecture of the generator and discriminator sub-networks of the proposed CR-GAN are described in Table 1 and Table 2 respectively. Conv1-Conv3 and Resnet block facilitate the extraction of noise-invariant features. (Note that Resnet Block followed by CRU denotes the combination of CRU post-ResNet Block, repeated nine times.) These features are upsampled into a binarized enhanced fingerprint image by Deconv1 and Deconv2. Discriminator network employs convolutional blocks Conv5-Conv9 to extract features at different scales so as to classify a given fingerprint image as real/fake. Introduction of CRU after each of these blocks in the generator and discriminator sub-networks offers the flexibility of modifying the channel weights such that the activation of important features is high and activation of redundant/less significant features is low.

Figure 3 shows the refinement of the channel weights at each convolutional block. Different convolutional block captures features at different scales. The introduction of a refinement unit after each convolutional block helps the model to effectively learn the correlation between channels and adapt the channel weights accordingly.



As a result, it provides the proposed model with the independence to enhance or deprecate activations of features corresponding to different scales. This characteristic refinement of channel weights in accordance with the importance of each feature at each convolutional block helps the proposed model to better preserve the relevant fingerprint features while running down the contractive and expansive pathways. This, in effect, boosts the localization power and, by consequence, enhancement the performance of the proposed CR-GAN. Detailed architecture of CR-GAN is provided in Table 1 and Table 2.

Block	Kernels	Size	Stride	Padding	Layers
Conv1	64	7	1	3	Conv. Layer + Batch Norm + ReLu
CRU	1	1	1	0	Adaptive Avg. Pooling + Conv. Layer + Batch Norm + Sigmoid
Conv2	128	3	2	1	Conv. Layer + Batch Norm + ReLu + Conv. Layer + Batch Norm
CRU	1	1	1	0	Adaptive Avg. Pooling + Conv. Layer + Batch Norm + Sigmoid
Conv3	256	3	2	1	Conv. Layer + Batch Norm + ReLu + Conv. Layer + Batch Norm
CRU	1	1	1	0	Adaptive Avg. Pooling + Conv. Layer + Batch Norm + Sigmoid
ResNet Block	256	3	2	1	Conv. Layer + Batch Norm + ReLu + Conv. Layer + Batch Norm
CRU	1	1	1	0	Adaptive Avg. Pooling + Conv. Layer + Batch Norm + Sigmoid
Deconv1	128	3	2	1	Conv. Layer + Batch Norm + ReLu + Conv. Layer + Batch Norm
CRU	1	1	1	0	Adaptive Avg. Pooling + Conv. Layer + Batch Norm + Sigmoid
Deconv2	64	3	2	1	Conv. Layer + Batch Norm + ReLu + Conv. Layer + Batch Norm
CRU	1	1	1	0	Adaptive Avg. Pooling + Conv. Layer + Batch Norm + Sigmoid
Conv4	1	7	1	3	Conv. Layer + Tanh

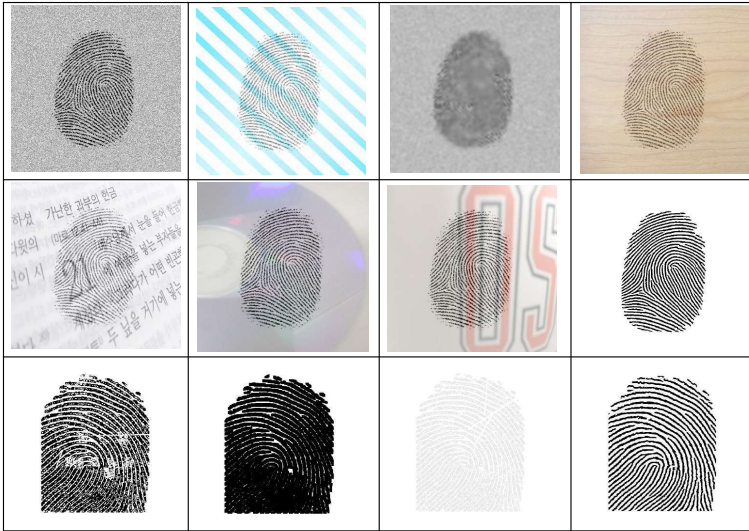
**Table 1** Architecture of generator network of the proposed CR-GAN.

### 3.3 Training

Training of CR-GAN requires paired data comprising degraded fingerprint images and the corresponding good quality enhanced images. However, the state-of-the-art fingerprint enhancement algorithms cannot generate reliable paired enhanced images (for poor quality input fingerprints) that can be used for training the proposed model. Another challenge is that there is only one rural fingerprint dataset available in the public domain. As a result, to have sufficient test cases for evaluating the performance of the proposed model, we create a synthetic degraded fingerprint database for training. Synthetic degraded fingerprint images are created from good quality fingerprint images (generated from a synthetic fingerprint generation tool [57]) by adding

Block	Kernels	Size	Stride	Padding	Layers
Conv5	64	4	2	1	Conv. Layer + LeakyReLU
CRU	1	1	1	0	Adaptive Avg. Pooling + Conv. Layer + Batch Norm + Sigmoid
Conv6	128	4	2	1	Conv. Layer + Batch Norm + LeakyReLU
CRU	1	1	1	0	Adaptive Avg. Pooling + Conv. Layer + Batch Norm + Sigmoid
Conv7	256	4	2	1	Conv. Layer + Batch Norm + LeakyReLU
CRU	1	1	1	0	Adaptive Avg. Pooling + Conv. Layer + Batch Norm + Sigmoid
Conv8	512	4	1	1	Conv. Layer + Batch Norm + LeakyReLU
CRU	1	1	1	0	Adaptive Avg. Pooling + Conv. Layer + Batch Norm + Sigmoid
Conv9	1	4	1	1	Conv. Layer

**Table 2** Architecture of discriminator network of the proposed CR-GAN.



**Fig. 4** Samples images from the synthetic dataset created to train the fingerprint enhancement model.

various noise, applying various morphological operations and blending with varying backgrounds. As shown in Figure 4, the synthetic training set captures noise patterns typically observed in degraded and poor quality fingerprint images. The paired enhanced images for the noisy training images is obtained by the binarization of the good quality fingerprint image by NBIS [7]. The fingerprint enhancement model is trained on 10500 synthetic fingerprints and corresponding ground-truth binarized images. The network is trained on Nvidia V100 GPU, adam optimizer with  $\lambda=10$ ,  $\beta_1=0.5$ ,  $\beta_2=0.999$ , learning rate=0.02 and batch size=2.

## 4 Experiments Evaluation

### 4.1 Databases

Degraded fingerprint impressions typically occur either due to poor skin conditions or due to background with structured noise. To analyze the performance of the proposed fingerprint enhancement model on poor quality fingerprints, we evaluate the proposed fingerprint enhancement model on two challenging rural fingerprint databases. For assessing the performance of the model on fingerprints with noisy background, we evaluate it on a latent fingerprint database. Details on all three databases is provided below.

1. **IIITD-MOLF [6]:** It is the most extensive publicly available latent database with 4400 latent fingerprints. The gallery fingerprints are acquired through the optical sensor from the same subjects.
2. **Rural Indian Fingerprint database [5]:** It is a publicly available database that comprises 1631 fingerprint images, with ten impressions of each finger. It contains samples from the rural population rigorously involved in manual work, including farmers, carpenters, villagers, etc.
3. **A private rural fingerprint database** comprising of 1000 fingerprint images. These images are acquired from 500 fingers using an optical fingerprint sensor. This database is especially challenging due to ample cases of the elderly population and degraded fingerprints.

### 4.2 Evaluation Metrics

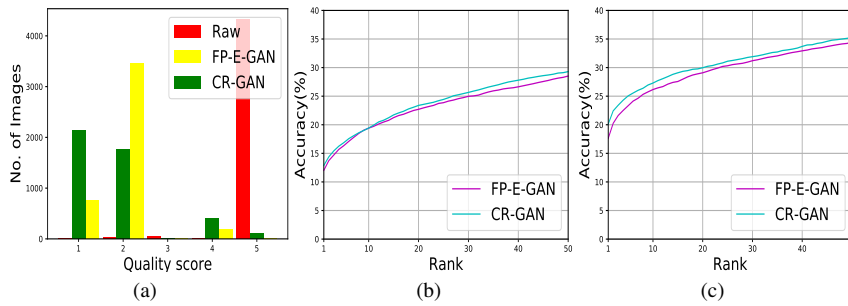
1. **Fingerprint Quality Assessment:** A fingerprint enhancement model is designed to improve fingerprint image quality. We use the *NFIQ* module of NBIS [7] to assess the fingerprint image quality of the enhanced images generated by the enhancement model. *NFIQ* outputs a score in the range 1-5, where 1 signifies the best and 5 signifies the worst quality. We acknowledge that *NFIQ2* [58] is a more robust fingerprint quality assessment metric. However, *NFIQ2* fails to process any of the three fingerprint image databases used in this research. As a result, we evaluate the quality of enhanced images using *NFIQ*.
2. **Ridge Structure Preservation:** One of the most critical characteristics of a fingerprint enhancement model is to preserve the fingerprint ridge details during enhancement. To quantify the ridge preservation aspect of the fingerprint enhancement algorithm, we calculate *SSIM* value [59] between the ground truth binarized fingerprint image and the output of the proposed CR-GAN. However, since the ground truth binarization cannot be reliably generated on the test datasets, we synthetically generate test cases of noisy images by adding various noise and background variations into good quality synthetic fingerprints obtained from [57]. The ground truth binarization is obtained from the good quality fingerprints using the binarization module of NBIS [7].
3. **Matching Performance:** The end goal of a fingerprint enhancement model is to facilitate improved matching performance. A fingerprint matching system may

operate in two different modes: identification and verification. The identification mode of operation is targeted to find a list of potential matches. Verification mode of operation, on the other hand, outputs where the input fingerprint matches with the gallery or not. We analyze the matching performance of reconstructed fingerprints in both modes of operation. Latent fingerprint matching is evaluated on an identification setting, so Rank-50 accuracy and cumulative matching characteristic (CMC) curves are plotted for IIITD-MOLF. However, rural fingerprint matching is evaluated in a verification setting. Hence, we report the average equal error rate (EER) and plot the detection error tradeoff (DET) curves. Fingerprint matching is performed using Bozorth [7] and MCC matcher [60], [61], [62], [63] (for both the matchers, minutiae are extracted using MINDTCT [7]).

## 5 Comparison with State-of-the-art

### 5.1 Performance on Latent Fingerprint Database

To establish the fact that the introduction of the proposed CRU into FP-E-GAN helps to learn more useful features, we compare the new architecture CR-GAN with FP-E-GAN on all the metrics as described in Section 4.2. Figure 5 (a) and Table 3 demonstrate that the average NFIQ score improves from 1.91 by FP-E-GAN to 1.77 by CR-GAN (lesser score indicates better quality). This illustrates the fact that channel



**Fig. 5** (Comparison of results on IIITD-MOLF database by FP-E-GAN and CR-GAN: (a) histogram of NFIQ scores; CMC curve comparing the identification performance obtained using (b) Bozorth (c) MCC

Enhancement Algorithm	Avg. NFIQ Score
Raw Image	4.96
FP-E-GAN [53]	1.91
<b>CR-GAN</b>	<b>1.77</b>

**Table 3** Comparison of average quality scores obtained using NFIQ on IIITD-MOLF database.

Enhancement Algorithm	Bozorth	MCC
Raw Image	5.45	6.06
Svoboda <i>et al.</i> [43]	NA	22.36
FP-E-GAN [53]	28.52	34.43
<b>CR-GAN</b>	<b>29.30</b>	<b>35.25</b>

**Table 4** Comparison of identification performance obtained on IIITD-MOLF database when matched across Lumidigm gallery.

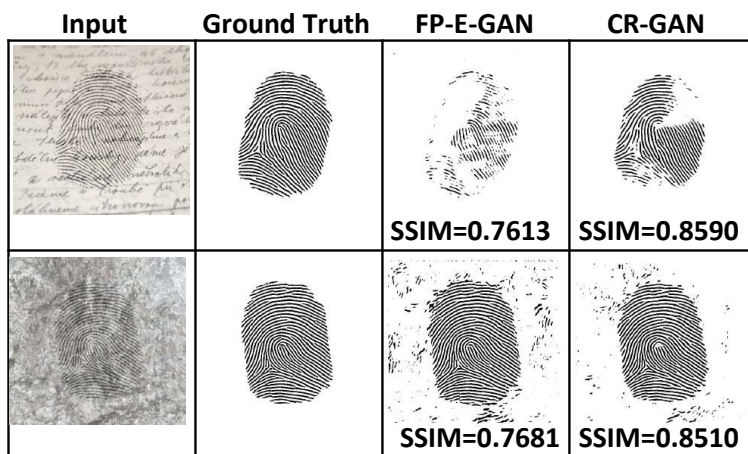


Fig. 6 Sample test cases comparing the ridge preservation ability of FP-GAN and CR-GAN.

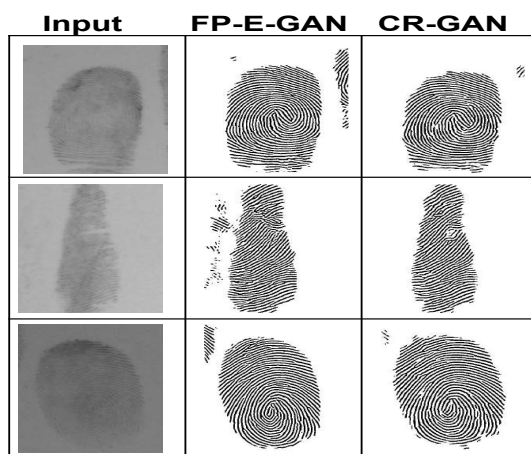


Fig. 7 Sample cases comparing the results of FP-E-GAN and CR-GAN on IIITD-MOLF database.

refinement helps CR-GAN to reconstruct better quality latent fingerprints than FP-E-GAN. Figure 6 and Table 4 demonstrate that CR-GAN outperforms FP-E-GAN on predicting missing/unclear ridge information and matching performance. Sample reconstructed fingerprints from IIITD-MOLF database are illustrated in the Figure 7 while the CMCs are plotted in Figure 5 (b) and (c). CR-GAN outperforms FP-E-GAN on all the three evaluation metrics as used in [53]. These results indicate that the introduction of the proposed CRU improves the latent fingerprint enhancement performance of the baseline FP-E-GAN. Next, we evaluate the performance of CR-GAN on rural fingerprints.

Enhancement Algorithm	Matching Algorithm	Avg. EER
Raw Image	Bozorth	16.36
STFT [28]	Bozorth	18.13
Hong <i>et al.</i> [22]	Bozorth	11.01
DeConvNet [41]	Bozorth	10.93
FP-E-GAN [53]	Bozorth	7.30
<b>CR-GAN</b>	Bozorth	<b>5.72</b>
Raw Image	MCC	13.23
STFT [28]	MCC	14.52
Hong <i>et al.</i> [22]	MCC	11.46
DeConvNet [41]	MCC	10.86
FP-E-GAN [53]	MCC	5.96
<b>CR-GAN</b>	MCC	<b>4.45</b>

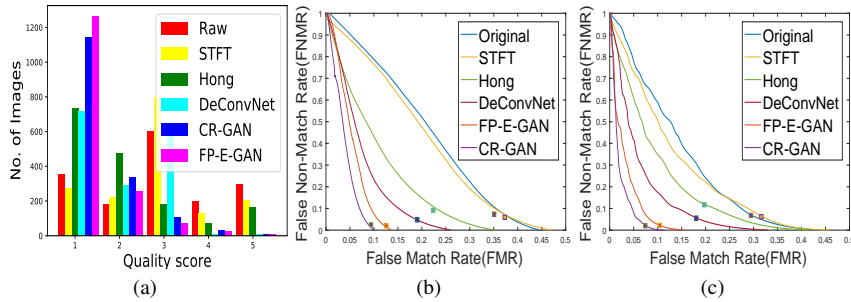
**Table 5** Average EER obtained on Rural Indian Fingerprint Database by various state-of-the-art fingerprint enhancement techniques.

Enhancement Algorithm	Avg. NFIQ Score
Raw Image	2.94
STFT [28]	2.86
Hong <i>et al.</i> [22]	2.05
DeconvNet [41]	1.95
<b>CR-GAN</b>	<b>1.42</b>
FP-E-GAN	<b>1.31</b>

**Table 6** Comparison of average NFIQ scores obtained on Rural Indian Fingerprint database.

Enhancement Algorithm	Matching Algorithm	Avg. EER
DeconvNet [41]	Bozorth	28.75
FP-E-GAN [53]	Bozorth	17.06
<b>CR-GAN</b>	Bozorth	<b>13.23</b>
DeconvNet [41]	MCC	26.80
FP-E-GAN [53]	MCC	15.85
<b>CR-GAN</b>	MCC	<b>11.52</b>

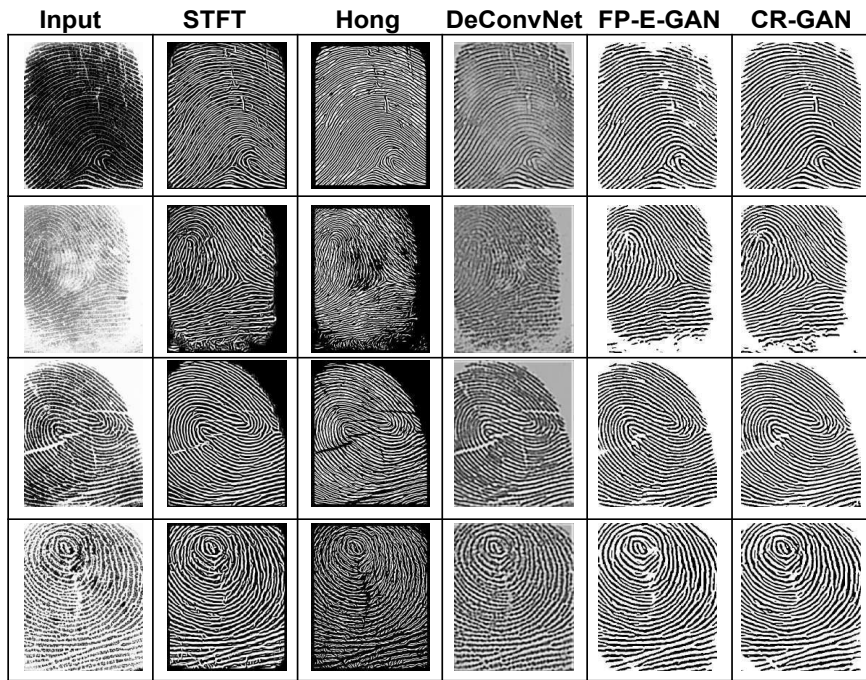
**Table 7** Average EER obtained on the private fingerprint database.



**Fig. 8** Comparison of state-of-the-art fingerprints enhancement schemes on the Rural Indian Fingerprint database: (a) histogram of NFIQ scores; DET curves obtained using (b) Bozorth (c) MCC

## 5.2 Comparison with State-of-the-art Fingerprint Enhancement Algorithms

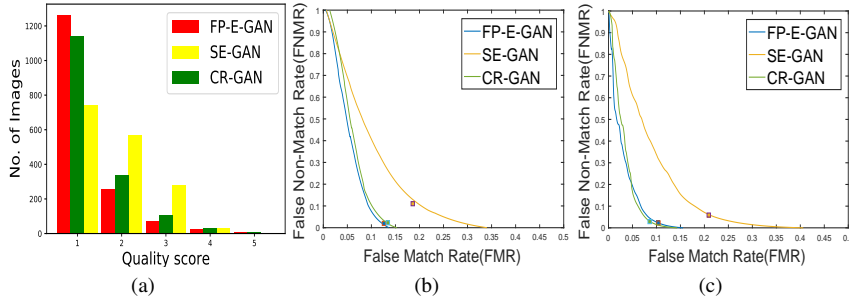
In order to compare the performance of the proposed CR-GAN, we benchmark state-of-the-art fingerprint enhancement algorithms: [22] (Hong), [28] (STFT), [41] (DeConvNet) and [53] (FP-E-GAN) on the rural Indian fingerprint databases described in Section 4.2. Fingerprint matching (verification) performance evaluated through



**Fig. 9** Sample cases of successful enhancement by CR-GAN (proposed) and comparison with the state-of-the-art fingerprint enhancement algorithms.

average equal error rate (EER) is reported in Table 5 and Table 7. Corresponding DET curves are plotted in Figure 8 (b) and (c). Average EER is significantly reduced across both the rural fingerprint databases irrespective of the choice of the fingerprint matching algorithm. This illustrates the fact that the proposed channel refinement unit improves the performance of FP-E-GAN [53]. As a result, CR-GAN outperforms the state-of-the-art enhancement algorithms on both datasets. These results verify the claim that some redundant channel weights are indeed learnt while training FP-E-GAN, and therefore, refinement of channel weights helps to improve the performance of FP-E-GAN. Next, we compare the fingerprint quality scores obtained by CR-GAN with state-of-the-art fingerprint enhancement algorithms. In Figure 8 (a), we plot the histogram of NFIQ values, while the average NFIQ score is reported in Table 6. Results show that the quality of enhanced fingerprints generated by CR-GAN is at par with FP-E-GAN, while matching performance is significantly improved.

Figure 9 illustrates sample restored fingerprint images obtained using the existing state-of-the-art fingerprint enhancement algorithms and the proposed CR-GAN. For all the sample inputs, CR-GAN outputs the smoothest ridges compared to the existing fingerprint enhancement algorithms. The first row depicts the case of high pressure while acquiring the fingerprint impression. As a result, very thick ridges are obtained, and valleys are not clearly visible. CR-GAN performs the best in predicting ridges and valleys and generates a fingerprint image with high ridge-valley clarity. The second row depicts the case of poor ridge clarity due to non-uniform pressure.



**Fig. 10** Comparison of SE-GAN and CR-GAN on the Rural Indian Fingerprint database: (a) histogram of NFIQ scores; DET curves obtained using (b) Bozorth (c) MCC

Model	Gen.	Disc.	Total
FP-E-GAN	11376129	2765505	14141634
<b>CR-GAN</b>	11383041	2768193	14151234
SE-GAN	12072081	3165177	15237258

**Table 8** Comparison of model parameters introduced by proposed channel refinement unit with SE-block [3].

Enhancement Algorithm	Avg. NFIQ Score	Enhancement Algorithm	Matching Algorithm	Avg. EER
SE-GAN	1.76	SE-GAN	Bozorth	12.34
<b>CR-GAN</b>	<b>1.42</b>	<b>CR-GAN</b>	Bozorth	<b>5.72</b>
		SE-GAN	MCC	10.50
		<b>CR-GAN</b>	MCC	<b>4.45</b>

**Table 9** Comparison of SE-block and the proposed channel refinement unit on NFIQ scores.

**Table 10** Comparison of SE-block and proposed channel refinement unit on average EER.

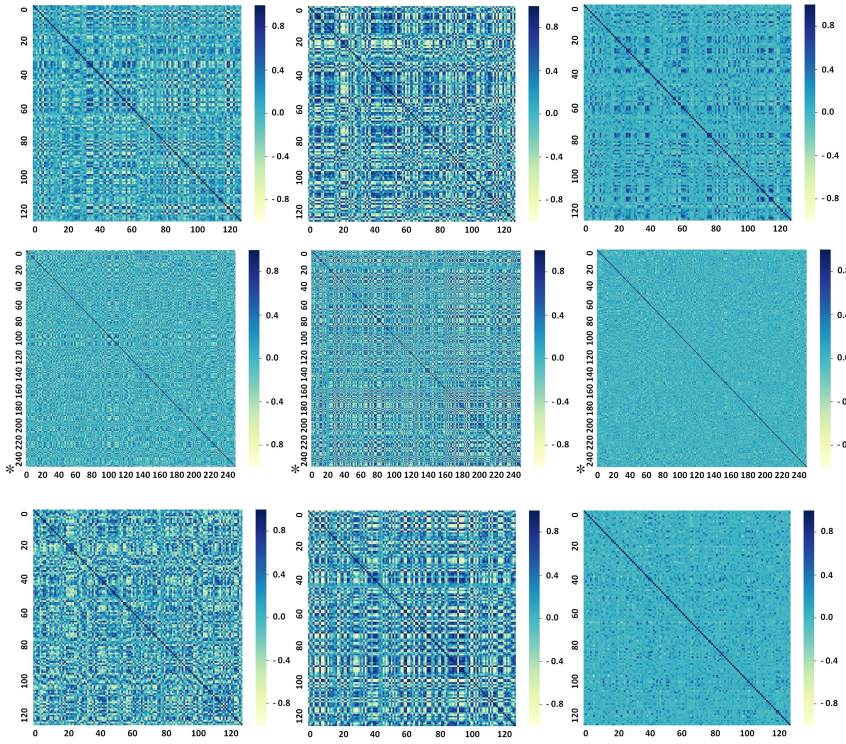
Unclear ridge details present in the input fingerprint image are correctly predicted by CR-GAN, while many of the state-of-the-art enhancement algorithms generate spurious ridge details. Likewise, in the third and fourth row, CR-GAN outperforms other algorithms in predicting the missing ridge details in the region where creases are present.

### 5.3 Comparison with Squeeze and Excitation block

This section compares the performance of the proposed CRU with the state-of-the-art channel-level attention mechanism Squeeze and Excitation (SE) block [3]. We replace the proposed CRU in the CR-GAN architecture with the SE block and refer to the resulting model as SE-GAN. In Table 8, we compare the number of parameters and observe that CR-GAN has lesser parameters than SE-GAN. This shows that the proposed CRU has lesser parameters compared to SE-block.

Table 9 compares the average fingerprint quality scores obtained by CR-GAN and SE-GAN. Figure 10 (a) presents the corresponding histogram of NFIQ values.

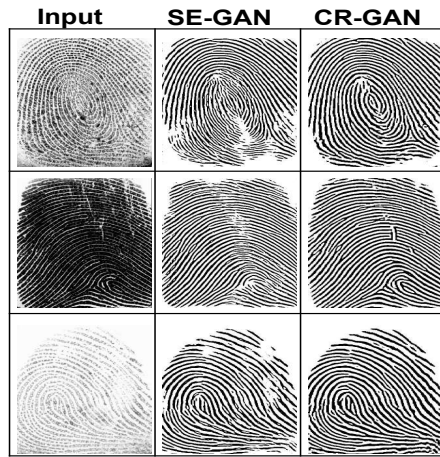




**Fig. 11** Comparison of correlation matrix obtained for channel weights of different layers in left to right: FP-E-GAN, SE-GAN, and CR-GAN. The first, second, and the third row represent layer numbers 3, 16, and 21, respectively, in FP-E-GAN (and corresponding layers in SE-GAN and CR-GAN).

Results show that the CR-GAN reconstructs better quality fingerprints compared to SE-GAN. To compare matching performance, average EER is reported in Table 10. Corresponding DET curves are plotted in Figure 10 (b) and (c). The average EER obtained by CR-GAN is significantly lesser compared to the SE-GAN for both the fingerprint matching algorithms. These results show that SE-block is not suited for fingerprint enhancement as the matching performance obtained by SE-GAN is inferior compared to the baseline FP-E-GAN. The proposed CR-GAN, on the other hand, outperforms SE-GAN and FP-E-GAN which demonstrates that the proposed CRU is well suited for fingerprint enhancement. These results also demonstrate the fact that the improved performance of CR-GAN cannot be simply attributed to increased model capacity as a result of the increased number of parameters in CR-GAN compared to FP-E-GAN. SE-GAN has more number parameters than CR-GAN, yet much inferior performance compared to FP-E-GAN. In order to analyze the effect of introducing the proposed CRU on features learnt by the model, we plot the correlation matrix between channel weights of layers of FP-E-GAN, SE-GAN, and CR-GAN in Figure 11.

A channel refinement technique is in principle designed to reduce redundancy among channel weights of the backbone network. However, we find that instead of

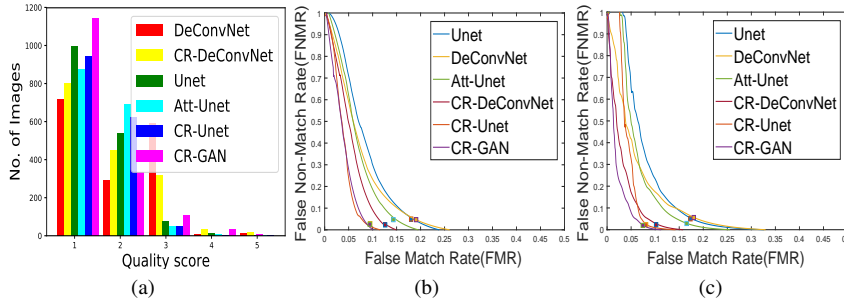


**Fig. 12** Sample cases comparing the reconstructed fingerprints obtained using SE-GAN and CR-GAN.

reduced correlation among channel weights, SE-GAN has higher correlation among channels as compared to the baseline FP-E-GAN. This shows that introduction of SE-block creates redundancy among features (high correlation values indicate high redundancy). CR-GAN, on the other hand, has the smallest correlation values. This indicates that the proposed channel refinement unit reduces redundancy among features and helps to learn robust features. Learning of more robust features by CR-GAN compared to FP-E-GAN and SE-GAN helps CR-GAN to outperform both FP-E-GAN and SE-GAN. Figure 12 compares sample restored fingerprint images obtained using proposed CR-GAN and SE-GAN. In all the cases, CR-GAN outperforms SE-GAN. CR-GAN reconstructs fingerprints with smoother ridges, higher ridge-valley clarity, and lesser spurious ridge features compared to SE-GAN.

#### 5.4 Generalization of Channel Refinement Unit to Different Choices of Network Architectures for Fingerprint Enhancement

So far, we observe that the introduction of the proposed CRU improves the performance of a generative adversarial network based fingerprint enhancement model. Next, we analyze whether the proposed CRU can generalize for different choices of network architectures for fingerprint enhancement. For this experiment, we take Unet [64] and DeConvNet [41] (an autoencoder based state-of-the-art fingerprint enhancement model) as the baseline network architectures. On both of these architectures, we introduce CRU after every convolution block (similar to CR-GAN) and develop new architectures called *CR-Unet* and *CR-DeConvNet* respectively. To assess whether the introduction of the proposed CRU improves the performance of Unet and DeConvNet, we compare the performance of CR-Unet and CR-DeConvNet with Unet and DeConvNet respectively. We also compare the performance of CR-Unet with spatial attention based Unet architecture called Attention Unet (Att-Unet) [65]. Imple-



**Fig. 13** Generalization of proposed channel refinement unit across state-of-the-art deep architectures (evaluated on the Rural Indian Fingerprint database): (a) histogram of NFIQ scores; DET curves obtained using (b) Bozorth (c) MCC

Enhancement Algorithm	Avg. NFIQ Score
DeconvNet [41]	1.95
<i>CR-DeConvNet</i>	1.78
Unet [64]	1.45
Att-Unet [65]	1.51
<i>CR-Unet</i>	1.45
<b>CR-GAN</b>	<b>1.42</b>

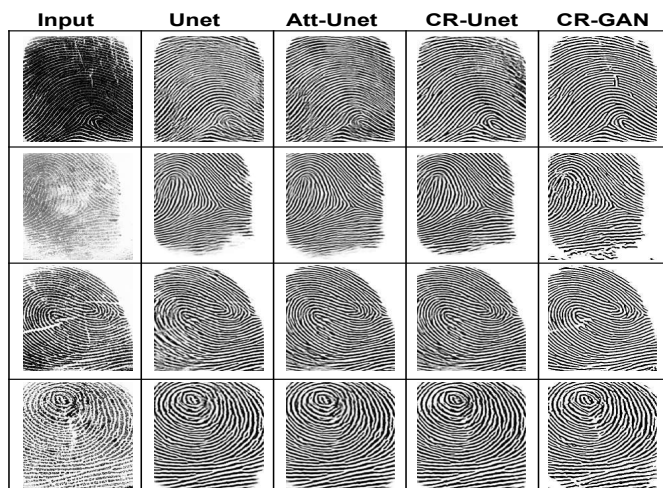
Enhancement Algorithm	Matching Algorithm	Avg. EER
Unet [64]	Bozorth	11.35
DeConvNet [41]	Bozorth	10.93
Att-Unet [65]	Bozorth	9.50
FP-E-GAN [53]	Bozorth	7.30
<i>CR-DeConvNet</i>	Bozorth	6.53
<i>CR-Unet</i>	Bozorth	5.99
<b>CR-GAN</b>	Bozorth	<b>5.72</b>
DeConvNet [41]	MCC	10.86
Unet [64]	MCC	10.58
Att-Unet [65]	MCC	9.08
FP-E-GAN [53]	MCC	5.96
<i>CR-Unet</i>	MCC	5.55
<i>CR-DeConvNet</i>	MCC	5.45
<b>CR-GAN</b>	MCC	<b>4.45</b>

**Table 11** Comparison of average NFIQ quality scores obtained (on Rural Indian Fingerprint database) by state-of-the-art deep architectures.

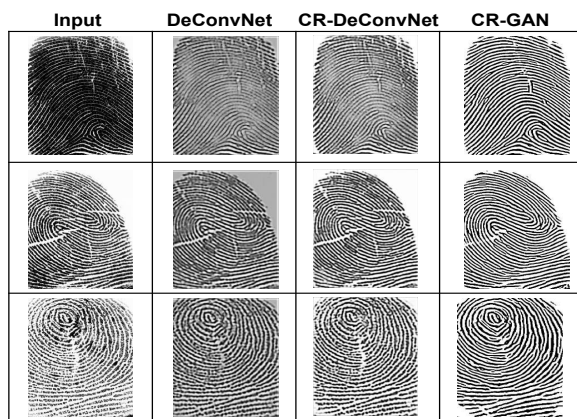
**Table 12** Average EER obtained on Rural Indian Fingerprint Database by various state-of-the-art deep architectures.

mentation of baseline Unet and Att-Unet are taken from [https://github.com/LeeJunHyun/Image\\_Segmentation](https://github.com/LeeJunHyun/Image_Segmentation).

First, we compare the fingerprint quality scores of the enhanced fingerprint images generated by different models. The average NFIQ score is reported in Table 11, while the histogram of NFIQ values is plotted in Figure 13 (a). Results verify the claim that the proposed CRU improves enhancement performance. The quality scores of fingerprints reconstructed by CR-Unet and CR-DeConvNet are better than Unet and DeConvNet respectively. Average EER obtained by all state-of-the-art deep architectures is reported in Table 12, while the corresponding DET curves are plotted in Figure 13 (b) and (c). For both the fingerprint matchers, average EER is significantly reduced. These results demonstrate the fact that redundant features are learnt by state-of-the-art deep architectures, when trained for fingerprint enhancement. The proposed CRU reduces redundancy among features and helps to learn robust features.



(a)



(b)

**Fig. 14** Samples showcasing the generalization ability of proposed channel refinement unit on (a) Unet and (b) DeConvNet architectures and comparison with proposed CR-GAN.

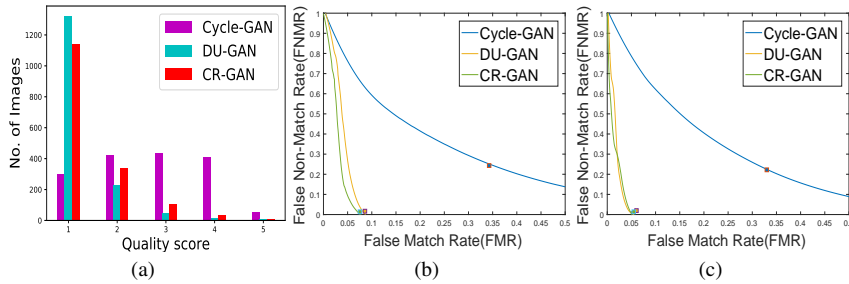
As a result, enhancement performance of CR-Unet and CR-DeConvNet turns out to be far better than Unet and DeConvNet respectively. All these results demonstrate the fact that the idea of introducing the proposed channel refinement unit generalizes over different state-of-the-art deep architectures.

We also observe that CR-Unet outperforms Att-Unet [65] by a significant margin. Att-Unet exploits spatial attention while CR-Unet exploits channel-level attention. The fact that CR-Unet outperforms Att-Unet on both fingerprint quality score and matching performance demonstrates that channel-level attention is more useful for fingerprint enhancement than spatial attention. Interestingly, we also observe that both CR-Unet and CR-DeConvNet architectures proposed for this experiment outperform FP-E-GAN. However, since the baseline performance of FP-E-GAN is

significantly better compared to the baseline performance of Unet and DeConvNet. As a result, the proposed CR-GAN outperforms CR-Unet and CR-DeConvNet. In Figure 14 (a), we compare the sample reconstructed fingerprints generated by Unet, Att-Unet, and CR-Unet. We find that the fingerprints generated by CR-Unet have better ridge-valley clarity and lesser spurious features compared to Unet and Att-Unet. Similar observations are noted when CR-DeConvNet is compared to DeConvNet, as shown in Figure 14 (b).

## 6 Comparison with State-of-the-art Generative Adversarial Network Based Fingerprint Enhancement Models

This section compares the performance of the proposed CR-GAN with the state-of-the-art generative adversarial network based fingerprint enhancement models CycleGAN [55] and DU-GAN [56]. Figure 15 (a) and Table 13 compare the average NFIQ fingerprint quality score obtained on enhanced images generated using CycleGAN, DU-GAN and the proposed CR-GAN. We find that the fingerprint quality of images generated by CR-GAN are significantly better than CycleGAN and competitive with DU-GAN. Figure 15 (b) and (c) and Table 14 present the average EER obtained by all the models. We find that CycleGAN is unable to preserve ridge structure during enhancement due to which it obtains unsatisfactory performance. Proposed CR-GAN on the other hand, obtains the best enhancement performance indicated by lowest EER compared to CycleGAN and DU-GAN.



**Fig. 15** Comparison of the proposed CR-GAN with state-of-the-art generative adversarial network based fingerprint enhancement models CycleGAN and DU-GAN on the Rural Indian Fingerprint database: (a) histogram of NFIQ scores; DET curves obtained using (b) Bozorth (c) MCC

Enhancement Algorithm	Avg. NFIQ Score
Cycle-GAN [55]	1.76
DU-GAN [56]	<b>1.26</b>
<b>CR-GAN</b>	1.42

**Table 13** Comparison of the NFIQ quality score obtained by the proposed CR-GAN, Cycle-GAN and DU-GAN.

Enhancement Algorithm	Matching Algorithm	Avg. EER
Cycle-GAN [55]	Bozorth	29.52
DU-GAN [56]	Bozorth	7.13
<b>CR-GAN</b>	Bozorth	<b>5.72</b>
Cycle-GAN [55]	MCC	27.96
DU-GAN [56]	MCC	5.13
<b>CR-GAN</b>	MCC	<b>4.45</b>

**Table 14** Comparison of the average EER obtained by the proposed CR-GAN, Cycle-GAN and DU-GAN.

## 7 Analysis of the Proposed Model

### 7.1 Ridge Structure Preservation





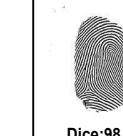







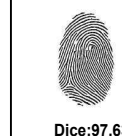


Various kinds of noise patterns can accompany a degraded input fingerprint. In order to quantify the ridge preservation ability of the proposed CR-GAN on different noise patterns observed in degraded input fingerprints, we calculate SSIM similarity scores between the ground truth binarized image and the output of CR-GAN corresponding to the given input. A high similarity score indicates that the model preserves ridge details viz. fingerprint pattern type, the orientation of ridges, and minutiae details of the input fingerprint image while enhancing them. Figure 16 presents sample degraded fingerprints (first column from left) and the enhanced images generated using CR-GAN (rightmost column). The second column represents the corresponding ground truth binarized fingerprint images. High similarity scores between the output of CR-GAN and ground truth are obtained, which demonstrates the fact that the proposed CR-GAN preserves the ridge structure of the input fingerprint while enhancing it.

### 7.2 Ablation Study

We also conduct an ablation study on the proposed CR-GAN to individually quantify the effect of introducing the proposed CRU on generator and discriminator sub-networks. We explore three different variants, when the proposed channel refinement

Refinement	Matching Algorithm	Avg. EER
Discriminator	Bozorth	7.68
Generator	Bozorth	6.79
Both	Bozorth	<b>5.72</b>
Discriminator	MCC	5.81
Generator	MCC	4.73
Both	MCC	<b>4.45</b>

**Table 15** Ablation Study: Average EER obtained on the Rural Indian Fingerprint Database through the application of proposed channel refinement on the GAN architecture.

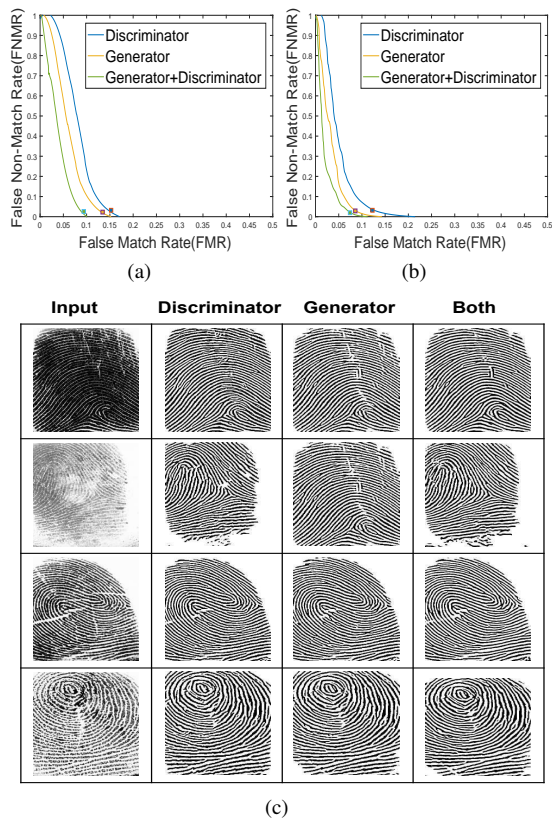
Input	Ground Truth	Discriminator	Generator	Both
		 Dice: 96.87 Jaccard: 94.60 SSIM: 85.16 PSNR: 12.63	 Dice: 97.99 Jaccard: 96.55 SSIM: 89.57 PSNR: 14.61	 Dice: 98.38 Jaccard: 97.30 SSIM: 90.96 PSNR: 15.50
		 Dice: 95.05 Jaccard: 90.61 SSIM: 75.52 PSNR: 12.44	 Dice: 95.95 Jaccard: 92.28 SSIM: 80.04 PSNR: 13.43	 Dice: 96.08 Jaccard: 92.51 SSIM: 81.06 PSNR: 13.55
		 Dice: 97.63 Jaccard: 95.92 SSIM: 88.08 PSNR: 13.85	 Dice: 98.33 Jaccard: 97.19 SSIM: 91.22 PSNR: 15.42	 Dice: 98.39 Jaccard: 97.28 SSIM: 91.51 PSNR: 15.58

**Fig. 16** Sample synthetic test cases illustrating the ridge preservation ability of CR-GAN and its variants used for the experiments on ablation study.

unit is applied: only the generator, only the discriminator, and both generator and discriminator. Average EER obtained for all the three variants is reported in Table 15 and the corresponding DET curves are plotted in Figure 17 (a) and (b). Sample reconstructions generated by all the three variants are shown in Figure 16 and Figure 17 (c). Results demonstrate the fact that channel refinement of the generator turns out to be more beneficial compared to the refinement of the discriminator, which makes sense as the generator is directly targeted to generate the enhanced image and therefore has a much deeper architecture, leading to much more redundant channel weights compared to the discriminator, which has a fairly smaller architecture and thus less redundant features. Furthermore, as expected, the best performance is obtained when channel weight refinement is applied on both the generator and discriminator sub-networks.

### 7.3 Successful Cases

Figure 18 illustrates some of the successful cases of enhancement by the proposed CR-GAN. The first and second columns (from left) are latent fingerprints and represent the case of unclear ridge structure due to the presence of non-uniform chemical

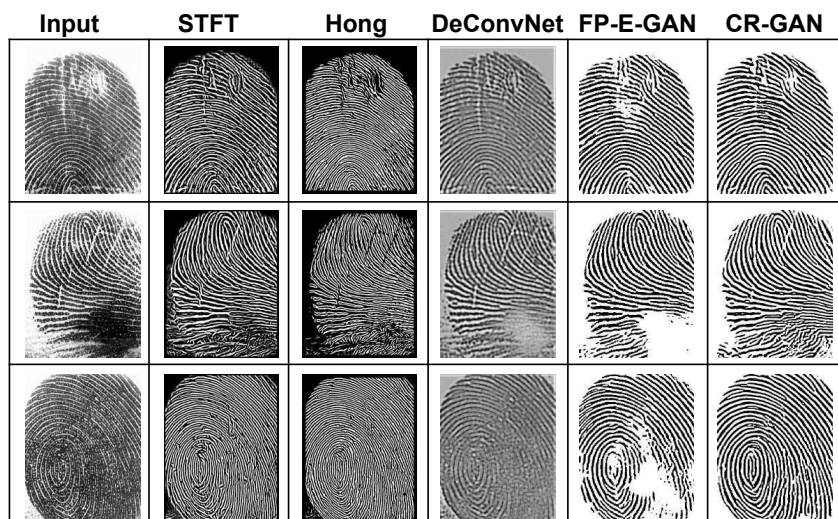


**Fig. 17** DET curves demonstrating the significance of the proposed Channel Refinement using (a) Bozorth (b) MCC. (c) Sample cases from the Rural Indian Fingerprint database showcasing the ablation study conducted on the proposed CR-GAN.



**Fig. 18** Sample successful reconstructions by the proposed CR-GAN.





**Fig. 19** Sample challenging cases and comparison with the state-of-the-art fingerprint enhancement algorithms.

powder (while lifting the latent fingerprint). In both cases, CR-GAN successfully reconstructs fingerprints with good ridge-valley clarity. The third column represents the scenario of unclear valleys due to thick ridges resulting from high pressure or wet finger. Once again, proposed CR-GAN correctly infers ridge and valley information and generates a good quality enhanced image. The fourth and fifth columns represent the case of missing ridge information due to creases or cuts. CR-GAN successfully predicts the missing ridge details in the region where creases and cuts are present.

#### 7.4 Challenging Cases

Figure 19 illustrates the performance of CR-GAN on some of the challenging cases. In the first row, near the scarred region, CR-GAN generates spurious ridge patterns. In the second row, around the region of high pressure, the ridges in the input fingerprint are too dark. As a result, CR-GAN generates non-smooth and spurious ridges. However, in all the cases, CR-GAN outperforms the baseline FP-E-GAN (and other state-of-the-art fingerprint enhancement models as well). This reaffirms the fact that refinement of channel weights improves the model performance, both qualitatively and quantitatively.

## 8 Conclusion

This paper illustrates that the refinement of channel weights improves the baseline FP-E-GAN's performance and the resulting model outperforms state-of-the-art fingerprint enhancement models. We also demonstrate that the proposed channel refinement unit is useful for simpler architectures such as Unet and DeConvNet as well.

We compare the proposed channel refinement unit to state-of-the-art channel level attention module SE-block and demonstrate that the improved performance cannot be simply attributed to increased model capacity. In the future, we plan to explore whether channel refinement can generalize over other modules of an automated fingerprint matching system as well.

## 9 Acknowledgement

The authors are grateful to Prof. Phalguni Gupta from IIT Kanpur for sharing the private rural Indian fingerprint database used in this research. The authors thank the HPC facility of Inria Sophia Antipolis for the computational resources used in this research. The authors acknowledge the efforts of Adithya Anand from IIT Delhi in preparing the training dataset. This work is partly supported by the French Government (National Research Agency, ANR) under grant agreement ANR-18-CE92-0024. I. Joshi is partially supported by the Raman-Charpak Fellowship 2019.

## References

1. Joshi I, Kothari R, Utkarsh A, Kurmi V K, Dantcheva A, Dutta Roy S and Kalra P K (2021) Explainable fingerprint roi segmentation using monte carlo dropout. In: Winter Conference on Applications of Computer Vision Workshops (WACVW), pp. 60-69. IEEE Computer Society
2. Joshi I, Utkarsh A, Kothari R, Kurmi V K, Dantcheva A, Dutta Roy S and Kalra P K (2021) Sensor-invariant fingerprint roi segmentation using recurrent adversarial learning. In: International Joint Conference on Neural Networks (IJCNN), pp. 1-8. IEEE
3. Hu J, Shen L and Sun G (2018) Squeeze-and-excitation networks. In: Conference on computer vision and pattern recognition, pp. 7132-7141. IEEE
4. Woo S, Park J, Lee J Y and So Kweon I (2018) Cbam: Convolutional block attention module. In: European conference on computer vision (ECCV), pp. 3-19. IEEE
5. Puri C, Narang K, Tiwari A, Vatsa M and Singh R (2010) On analysis of rural and urban Indian fingerprint images. In: International Conference on Ethics and Policy of Biometrics, pp. 55-61. Springer
6. Sankaran A, Vatsa M and Singh R (2015) Multisensor optical and latent fingerprint database. IEEE access 3:653-665
7. NIST Biometric Image Software (2015). <http://www.nist.gov/itl/iad/ig/nbis.cfm>. Accessed: 4 December 2020
8. Vaswani A, Shazeer N, Parmar N, Uszkoreit J, Jones L, Gomez A N and Polosukhin I (2017) Attention is all you need. In: Advances in neural information processing systems, pp. 5998-6008
9. Mnih V, Heess N and Graves A (2014) Recurrent models of visual attention. In: Advances in neural information processing systems, pp. 2204-2212
10. Park J, Woo S, Lee J Y and Kweon I S (2018) Bam: Bottleneck attention module. arXiv preprint arXiv:1807.06514
11. Hu J, Shen L, Albanie S, Sun G and Vedaldi A (2018) Gather-excite: Exploiting feature context in convolutional neural networks. In: Advances in neural information processing systems, pp. 9401-9411
12. Huang Z, Wang X, Huang L, Huang C, Wei Y, Liu W (2019) Ccnet: Criss-cross attention for semantic segmentation. In: Conference on computer vision and pattern recognition, pp. 603-612. IEEE
13. Singh P, Mazumder P and Nambodiri V P (2020) Accuracy booster: performance boosting using feature map re-calibration. In: Winter Conference on Applications of Computer Vision (WACV), pp. 884-893. IEEE
14. Bello I, Zoph B, Vaswani A, Shlens J, Le Q V (2019) Attention Augmented Convolutional Networks. In: International Conference on Computer Vision, pp. 3286-3295. IEEE
15. Wang F, Jiang M, Qian C, Yang S, Li C, Zhang H, Wang X, and Tang X (2017) Residual attention network for image classification. In: Conference on computer vision and pattern recognition, pp. 3156-3164. IEEE

16. Chen L, Zhang H, Xiao J, Nie L, Shao J, Liu W, and Chua T S (2017) Sca-cnn: Spatial and channel-wise attention in convolutional networks for image captioning. In: Conference on computer vision and pattern recognition, pp. 5659-5667. IEEE
17. Roy R, Joshi I, Das A, Dantcheva A (200) 3D CNN Architectures and Attention Mechanisms for Deepfake Detection. arXiv preprint hal.archives-ouvertes.fr: hal-03524639 (accepted for publication in Handbook of Digital Face Manipulation and Detection, Springer)
18. Jia F, Ma L, Yang Y and Zeng T (2021) Pixel-Attention CNN With Color Correlation Loss for Color Image Denoising. IEEE Signal Processing Letters 28:1600-1604
19. Li D, Wen G, Kuai Y and Porikli F (2018) End-to-end feature integration for correlation filter tracking with channel attention. IEEE Signal Processing Letters 25(12):1815-1819
20. Vatsa M, Singh R, Bharadwaj S, Bhatt H, and Mashruwala R (2010) Analyzing fingerprints of Indian population using image quality: A UIDAI case study. In: International Workshop on Emerging Techniques and Challenges for Hand-Based Biometrics, pp. 1-5. IEEE
21. Tiwari K and Gupta P (2014) Fingerprint quality of rural population and impact of multiple scanners on recognition. In: Chinese Conference on Biometric Recognition, pp. 199-207. Springer
22. Hong L, Wan Y and Jain A (1998) Fingerprint image enhancement: algorithm and performance evaluation. IEEE transactions on pattern analysis and machine intelligence 20(8):777-789
23. Gottschlich C and Schönlieb C B (2012) Oriented diffusion filtering for enhancing low-quality fingerprint images. IET biometrics 1(2):105-113
24. Turrone F, Cappelli R and Maltoni D (2012) Fingerprint enhancement using contextual iterative filtering. In: International Conference on Biometrics (ICB), pp. 152-157. IEEE
25. Ramos R C, de Lima Borges E V C, Andrezza I L P, Primo J J B, Batista L V and Gomes H M (2018) Analysis and improvements of fingerprint enhancement from gabor iterative filtering. In: SIBGRABI Conference on Graphics, Patterns and Images, pp. 266-273. IEEE
26. Wang W, Li J, Huang F and Feng H (2008) Design and implementation of log-gabor filter in fingerprint image enhancement. Pattern Recognition Letters 29(3):301-308
27. Gottschlich C (2011) Curved-region-based ridge frequency estimation and curved gabor filters for fingerprint image enhancement. IEEE Transactions on Image Processing 21(4):2220-2227
28. Chikkerur S, Cartwright A N and Govindaraju V (2007) Fingerprint enhancement using stft analysis. Pattern recognition 40(1):198-211
29. Hsieh C T, Lai E and Wang Y C (2003) An effective algorithm for fingerprint image enhancement based on wavelet transform. Pattern Recognition 36(2):303-312
30. Ghafoor M, Taj I A, Ahmad W and Jafri N M (2014) Efficient 2-fold contextual filtering approach for fingerprint enhancement. IET Image Processing 8(7):417-425
31. Jirachaweng S and Areekul V (2007) Fingerprint enhancement based on discrete cosine transform. In: International Conference on Biometrics, pp. 96-105. Springer
32. Yoon S, Feng J and Jain A K (2010) On latent fingerprint enhancement. In: Biometric Technology for Human Identification VII 7667:766707. International Society for Optics and Photonics
33. Gupta R, Khari M, Gupta D and Crespo R G (2020) Fingerprint image enhancement and reconstruction using the orientation and phase reconstruction. Information Sciences 530:201-218
34. Le N T, Wang J W, Le D H, Wang C C and Nguyen T N (2020) Fingerprint enhancement based on tensor of wavelet subbands for classification. IEEE Access 8: 6602-6615
35. Manickam A, Devarasan E, Manogaran G, Priyan M K, Varatharajan R, Hsu C H and Krishnamoorthi R (2019) Score level based latent fingerprint enhancement and matching using SIFT feature. Multimedia Tools and Applications 78(3):3065-3085
36. Yang X, Feng J and Zhou J (2014) Localized dictionaries based orientation field estimation for latent fingerprints. IEEE transactions on pattern analysis and machine intelligence 36(5):955-969
37. Chen C, Feng J and Zhou J (2016) Multi-scale dictionaries based fingerprint orientation field estimation. In: International Conference on Biometrics (ICB), pp. 1-8. IEEE
38. Liu S, Liu M and Yang Z (2017) Sparse coding based orientation estimation for latent fingerprints. Pattern Recognition 67:164-176
39. Xu D, Bian W, Cheng Y, Li Q, Luo Y and Yu Q (2020) Fingerprint enhancement using multi-scale classification dictionaries with reduced dimensionality. IET Biometrics 9(5):194-204
40. Sahasrabudhe M and Nambodiri A M (2014) Fingerprint enhancement using unsupervised hierarchical feature learning. In: Indian Conference on Computer Vision Graphics and Image Processing, pp. 1-8. ACM
41. Schuch P, Schulz S and Busch C (2016) De-convolutional autoencoder for enhancement of fingerprint samples. In: International Conference on Image Processing Theory, Tools and Applications (IPTA), pp. 1-7. IEEE

42. Rama R K and Namboodiri A M (2011). Fingerprint enhancement using hierarchical markov random fields. In: International Joint Conference on Biometrics (IJCB), pp. 1-8. IEEE
43. Svoboda J, Monti F and Bronstein M M (2017). Generative convolutional networks for latent fingerprint reconstruction. In: International Joint Conference on Biometrics (IJCB), pp. 429-436. IEEE
44. Horapong K, Srisutheanon K and Areekul V (2021). Progressive and corrective feedback for latent fingerprint enhancement using boosted spectral filtering and spectral autoencoder. IEEE Access
45. Qian P, Li A, and Liu M (2019) Latent fingerprint enhancement based on densenet. In: International Conference on Biometrics (ICB), pp. 1-6. IEEE
46. Liu M and Qian P (2020) Automatic segmentation and enhancement of latent fingerprints using deep nested unets. IEEE Transactions on Information Forensics and Security 16:1709-1719
47. Wong W J and Lai S H (2020) Multi-task CNN for restoring corrupted fingerprint images. Pattern Recognition 101:107203
48. Li J, Feng J and Kuo C C J (2018) Deep convolutional neural network for latent fingerprint enhancement. Signal Processing: Image Communication 60:52-63
49. Sharma R P and Dey S (2019) Two-stage quality adaptive fingerprint image enhancement using fuzzy c-means clustering based fingerprint quality analysis. Image and Vision Computing 83:1-16
50. Joshi I, Utkarsh A, Kothari R, Kurmi V K, Dantcheva A, Dutta Roy S and Kalra P K (2022) On Estimating Uncertainty of Fingerprint Enhancement Models. In: Digital Image Enhancement and Reconstruction. Elsevier (accepted)
51. Medeiros A G, Andrade J P, Serafim P B, Santos A M, Maia J G, Trinta F A, Macedo J A, Fileho P P and Rego P A (2020) A Novel Approach for Automatic Enhancement of Fingerprint Images via Deep Transfer Learning. In: International Joint Conference on Neural Networks (IJCNN), pp. 1-8. IEEE
52. Schuch P, Schulz S and Busch C (2017) Survey on the impact of fingerprint image enhancement. IET Biometrics 7(2):102-115
53. Joshi I, Anand A, Vatsa M, Singh R, Dutta Roy S and Kalra P (2019) Latent fingerprint enhancement using generative adversarial networks. In: Winter Conference on Applications of Computer Vision (WACV), pp. 895-903. IEEE
54. Joshi I, Anand A, Dutta Roy S and Kalra P K (2021) On training generative adversarial network for enhancement of latent fingerprints. In: AI and Deep Learning in Biometric Security, pp. 51-79. CRC Press
55. Karabulut D, Tertychnyi P, Arslan H S, Ozcinar C, Nasrollahi K, Valls J, Vilaseca J, Moeslund T B and Anbarjafari G (2020). Cycle-consistent generative adversarial neural networks based low quality fingerprint enhancement. Multimedia Tools and Applications 79(25):18569-18589
56. Joshi I, Utkarsh A, Kothari R, Kurmi V K, Dantcheva A, Dutta Roy S and Kalra P K (2021) Data uncertainty guided noise-aware preprocessing of fingerprints. In: International Joint Conference on Neural Networks (IJCNN), pp. 1-8. IEEE
57. Ansari A H (2011) Generation and storage of large synthetic fingerprint database. Dissertation, Indian Institute of Science Bangalore
58. NFIQ 2.0: NIST Fingerprint image quality (2016).<https://www.nist.gov/services-resources/software/development-nfiq-20>. Accessed: 8 December 2020
59. Wang Z, Bovik A C, Sheikh H R and Simoncelli E P (2004) Image quality assessment: from error visibility to structural similarity. IEEE transactions on image processing 13(4):600-612
60. Cappelli R, Ferrara M and Maltoni D (2010) Minutia cylinder-code: A new representation and matching technique for fingerprint recognition. IEEE transactions on pattern analysis and machine intelligence 32(12):2128-2141
61. Cappelli R, Ferrara M and Maltoni D (2010) Fingerprint indexing based on minutia cylinder-code. IEEE transactions on pattern analysis and machine intelligence 33(5):1051-1057
62. Ferrara M, Maltoni D and Cappelli R (2012) Noninvertible minutia cylinder-code representation. IEEE Transactions on Information Forensics and Security 7(6):1727-1737
63. Ferrara M, Maltoni D and Cappelli R (2014) A two-factor protection scheme for MCC fingerprint templates. In: International Conference of the Biometrics Special Interest Group (BIOSIG), pp. 1-8. IEEE
64. Ronneberger O, Fischer P and Brox T (2015) U-net: Convolutional networks for biomedical image segmentation. In: International Conference on Medical image computing and computer-assisted intervention, pp. 234-241. Springer
65. Oktay O, Schlemper J, Folgoc L L, Lee M, Heinrich M, Misawa K and Glocker B (2018) Attention u-net: Learning where to look for the pancreas. arXiv preprint arXiv:1804.03999